

# Multiresolution texture models for brain tumor segmentation in MRI

Khan M. Iftekharruddin, Shaheen Ahmed and Jakir Hossen

**Abstract**– In this study we discuss different types of texture features such as Fractal Dimension (FD) and Multifractional Brownian Motion (mBm) for estimating random structures and varying appearance of brain tissues and tumors in magnetic resonance images (MRI). We use different selection techniques including KullBack – Leibler Divergence (KLD) for ranking different texture and intensity features. We then exploit graph cut, self organizing maps (SOM) and expectation maximization (EM) techniques to fuse selected features for brain tumors segmentation in multimodality T1, T2, and FLAIR MRI. We use different similarity metrics to evaluate quality and robustness of these selected features for tumor segmentation in MRI for real pediatric patients. We also demonstrate a non-patient-specific automated tumor prediction scheme by using improved AdaBoost classification based on these image features.

## I. INTRODUCTION

Brain tissue and tumor segmentation in MR images has been an active research area. Extraction of good features is fundamental to successful image segmentation. Due to complex structures of different tissues such as the gray matter (GM), white matter (WM) and cerebrospinal fluid (CSF) in the MR brain images, extraction of useful features is a challenging task. Intensity is an important feature in segmenting tumor from other tissues in the brain. In Ref. [1], the authors use intensity and a conventional fuzzy c-means clustering algorithm for segmentation of CSF, GM and WM in MR images. An unsupervised MR image segmentation method based on self organizing maps (SOM) is proposed in [2]. However, using intensity alone for segmentation has proved to be insufficient. Fractal Dimension (FD) is a useful tool to characterize the textured images and surface roughness [3]. In several of our previous works [4, 5, 11-14, 16, 17], we demonstrated the effectiveness of fractal features in characterizing brain tumor tissue. Furthermore, we effectively analyzed the irregular texture variations of tumors in MRI using multifractal Brownian motion (mBm) for robust brain tumor segmentation [5]. On the other hand, researchers have used feature selection in many applications such as medical imaging, data mining and lexical works [6-7]. The authors in Ref. [8] develop a novel algorithm for normalizing the intensities of an image to best match those of a model distribution. In Ref. [9], the authors perform KLD across image modalities, including structural MRI, functional MRI and EEG data for fusion. The authors discuss a new feature selection technique based on KLD between two-class conditional densities functions approximated by finite mixture of parameterized densities in

[10]. In this work, we show comparative efficacy of different multiresolution texture models to segment brain tumors in pediatric T1, T2, and FLAIR MRI respectively. We further show results of feature fusion for generating a patient independent classifier for tumor detection and prediction.

## II. BACKGROUND REVIEW

In this section, we first review relevant background for feature extraction using fractal and multifractal texture methods. In our previous works [11-13], we discuss the usefulness of intensity, FD and mBm wavelet fractal texture features for tumor segmentation. In this work, we explore effectiveness of three different feature fusion and segmentation techniques such as EM, SOM and graph cut respectively [14].

### A. Fractal Dimension (FD) texture feature extraction

The concept of fractal is first proposed by Mandelbrot [15] to describe the geometry of the objects in nature. The FD is a real number that characterizes the fractalness (texture) of the objects. We investigate effectiveness of three different FD computation methods for brain tumor segmentation in MRI [11]. In a prior work [16], we demonstrate that piecewise-triangular-prism-surface-area (PTPSA) method offers the most reliable FD values and resulting tumor segmentation.

### B. Multifractional Brownian Motion (mBm) texture feature extraction

We successfully investigated mBm-based texture model for brain tumor segmentation in MRI [6]. The mBm is defined as,

$$x(at) = a^{H(t)} x(t) \quad (1)$$

where  $x(t)$  is an mBm process,  $H(t)$  is the time varying scaling (or Holder) exponent and  $a$  is the scaling factor. After a sequence of mathematical derivation, For 2-D mBm model, let  $\vec{z}(u)$  represent a 2D mBm process, where  $\vec{u}$  denotes the vector position ( $u_x, u_y$ ) of a point in the process. We can approximate  $H(\vec{u})$  for a 2D mBm process as follows [6],

$$2H(\vec{u}) = \lim_{a \rightarrow 0} \frac{\log\left(\frac{1}{M+N} \sum_{x=0}^{N-1} \sum_{y=0}^{M-1} |W_z(b_{x,y}, a)|^2\right)}{\log a} \quad (2)$$

The Eqn. that links  $H(\vec{u})$  with FD is given as,

$$FD = E+1-H \quad (3)$$

where, E is Euclidean Dimension of the space of fractal (E = 2 for 2D image) and H is the Hurst coefficient.

### C. Kullback – Leibler Divergence for Feature selection & Entropy for feature ranking

The Kullback – Leibler Divergence (KLD) is a measure of difference between two probability distributions [10]. Therefore, KLD can be used for multivariate normal distributions, approximated for the class conditional distributions of the tumor and non-tumor regions in MR brain images. We exploit the idea of information theory such as mutual information and KLD for feature ranking and selection. The mutual information can also be understood as the expectation of the KLD of the univariate distribution  $p(x)$  of  $x$  from the conditional distribution  $p(x|c)$  of  $x$  given  $c$ .

### D. Brain Tumor Segmentation

We study three different segmentation techniques for comparison. For graph cut method [9], the image is considered a graph and nodes  $i$  and  $j$  are pixels. Note the edge weight  $W_{ij}$  denotes a local measure of similarity between two pixels. Let  $G = \{V, E\}$  where  $V$  stands for the node and  $E$  for edges. For EM algorithm, at each pixel in an image, we compute a d-dimensional feature vector that encapsulates intensity and texture information. EM algorithm assumes that a segment is chosen with a probability, and models the density associated with that segment as a Gaussian probability distribution function, with parameters  $(\mu, \sigma)$ , that depend on the chosen segment. This is known as a Gaussian mixture model. The EM tool yields the cluster mean and covariance, for a user-defined number of clusters and number of iterations. Finally, self-organizing maps (SOM) neural network can be used as segmentation tools. The SOM map consists of a regular grid unit which learns to represent the statistical data described by model vectors  $x \in R^n$ , where  $R^n$  represents n dimension real space. Each map unit  $i$  contains a vector  $m_i$  ( $m_i \in R^n$ ) that is used to represent the data [14].

### E. Similarity Coefficient (SC) for segmentation quality and robustness identification

For estimating the robustness of segmentation we consider different similarity measures such as Jaccard, Dice, Sokal & Sneath (SS) and Russel and Rao (RR) [17]. We quantify segmentation robustness by measuring the overlap of tumor using different similarity metrics such as Jaccard ( $p/p+q$ ), Dice ( $2p/2p+q$ ), SS ( $p/p+2r$ ) and RR ( $p/p+q+r$ ), where  $p$  is the area of tumor region in MRI (tumors segmented by radiologist and used as ground truth),  $q$  is the area of the tumor region segmented using EM algorithm and  $r$  is the non-tumor region.

## III. METHOD

The first step includes the preprocessing stage that minimizes intensity and inhomogeneity bias using a normalization algorithm. After preprocessing step, we extract four features such as intensity, shape, FD using

PTPSA algorithm, and mBm using fractal-wavelet algorithm in multimodality MR images. We use both KLD and the entropy measures for feature ranking and selection. The features selected are then used for the segmentation of the tumor region in MRI using EM. Finally, we propose a modified version of the AdaBoost to improve tumor classification rate. The first modification is the weights of the component classifier are calculated considering three factors such as (i) how many samples are correctly classified, (ii) how confidently the samples are classified with the current ensembles of classifiers and (iii) how difficult or informative the correctly classified samples are. The other proposed modification is we update the weights (probability of being selected in the next cycle) for each samples considering how confidently the samples are classified/misclassified in the current cycle. This modification helps the component classifier to concentrate more on difficult –to-classify patterns during prediction as well as training.

We propose a few novel modifications in Adaboost as shown in Fig. 1. The first modification in step 3(d) obtains the weights of the component classifiers. These weights are calculated considering three factors such as (i) how many samples are correctly classified, (ii) how confidently the samples are classified with the current ensemble of classifiers, and (iii) how difficult or informative the correctly classified samples are. The other proposed modification is shown in step 3(e). We update the weights (probability of being selected in the next cycle) for each training samples considering how *confidently* the samples are classified/misclassified in the current cycle. This modification helps the component classifier to concentrate more on difficult-to-classify patterns during prediction as well as in training. The prediction decision on a new sample  $x$  can be based on the weighted vote of the component

classifiers,  $H(x) = \frac{1}{k_{\max}} \sum_{k=1}^{k_{\max}} \alpha_k h_k(x)$ , where  $h(x)$  is class decision from each component classifiers and  $H(x)$  is the final decision.

$n$ : number of samples (patterns) in the training set

$\bar{x}$ : training samples,  $[x_1, x_2, \dots, x_n]$

$\bar{y}$ : class labels of the training samples,  $[y_1, y_2, \dots, y_n]$

$k_{\max}$ : maximum number of classifier

$W_k$ : weight distribution of the samples at iteration  $k$ ,  $[W_k(1), W_k(2), \dots, W_k(n)]$

1. initialize weights,  $W_1(i) = 1/n, i = 1, \dots, n$

2. set  $k = 1$

3. while  $k < k_{\max}$  do

a. increment,  $k = k + 1$

b. train component classifier  $C_k$  using training set sampled from  $\bar{x}$  according to  $W_k$

c. draw a test set of size  $n$  from  $\bar{x}$  according to  $W_k$  and computer the posterior probabilities  $prob(y_i | x_i)$

d. calculate the classifier weight,  $\alpha_k = \sum_{i=1}^n \beta_i$ , where,

$$\beta_i = \begin{cases} \text{prob}(y_i | x_i) W_k(i) & \text{iff } \text{prob}(y_i | x_i) \geq \text{prob}(y_j | x_i) \text{ for } \forall j \\ 0 & \text{otherwise} \end{cases}$$

e. update weight,

$$W_{k+1}(i) = W_k(i) \times \begin{cases} e^{-\text{prob}(y_i | x_i)} & \text{iff } \text{prob}(y_i | x_i) \geq \text{prob}(y_j | x_i) \text{ for } \forall j \\ e^{\text{prob}(y_i | x_i)} & \text{otherwise} \end{cases}$$

$$W_{k+1}(i) = \frac{W_{k+1}(i)}{\sum_{j=1}^n W_{k+1}(j)}$$

normalize weights,

4. return  $C_k$  and the corresponding weights  $\alpha_k$
5. end

Fig. 1 Proposed modified AdaBoost algorithm

#### IV. RESULTS & DISCUSSION

##### A. Feature Extraction and Selection

We first divide the images into 8 X 8 sub – images and obtain the corresponding features using PTPSA and mBm set algorithms respectively. We then obtain the normalized mean value of the FD, mBm, intensity and shape features for both tumor and non-tumor regions for each MRI slice. Finally, we obtain KLD plots for all the three MR image modalities per patient. Figure 2 shows results in T1, T2 and FLAIR modalities for patient #8 as an example. Figures 2(a) and (c) show that as the entire tumor cluster is located in the mBm plane. Thus, mBm can be used to effectively discriminate between the PF tumors and non-tumor tissues in T1 and FLAIR MRI. Figures 2(b) shows that intensity is necessary to isolate tumor cluster in T2. This similar trend is noted for all the ten patients in our database. Fig.2 clearly provides more effective separation of tumor features.

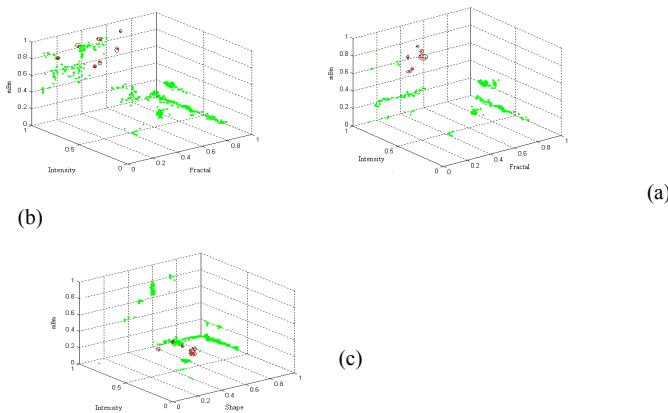


Fig. 2 KLD results showing the separability of features for (a) T1 modality; (b) T2 modality; (c) FLAIR modality for patient#8. Encircled dots show tumors and the rest shows non –tumor.

We compute the entropy values for all ten patients. Our entropy values for the feature matches with the KLD plots.

##### B. PF Tumor segmentation using selected MRI features

For effective comparison and evaluation, we employ three different tumor segmentation techniques such as SOM, graph cut and EM. Figure 3 shows tumor location in different modalities. Figure 4 shows an example for patient #8 in three MRI modalities.

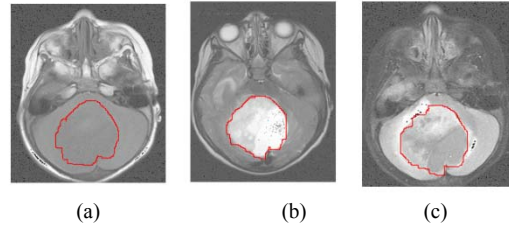


Fig. 3 An example MRI slice for (a) T1 modality; (b) T2 modality; (c)FLAIR modality for patient #8. Tumors have been shown using boundary.

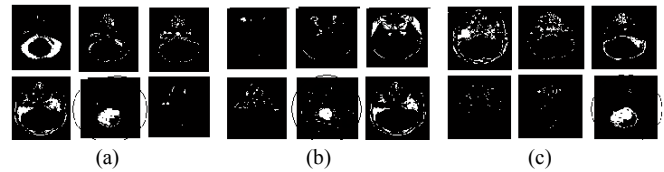


Fig. 4 Tumor segmentation using EM for patient #8 in (a) T1 image using mBm, (b) T2 image using intensity, (c) FLAIR image using mBm, respectively. Tumor segments are circled.

##### C. PF Tumor segmentation efficacy

Figure 5 shows radar plots for four similarity metrics such as Jaccard, Dice, (SS), and (RR) in T1, T2, and FLAIR modalities for all ten patients, respectively. In each subplot, for a specific metric the values in y-axis represent the overlap coefficient while the axis at each clock location represents the patient number. In Fig. 5(a) and (d), both the overall Jaccard and RR overlap is about 60% for all patients. We observe that the Dice overlap in Fig. 8(b) is above 80% for all patients. In Fig. 5(c), SS overlap for nine patients is above 60% except for a dip at 47% for patient #1 for all modalities.

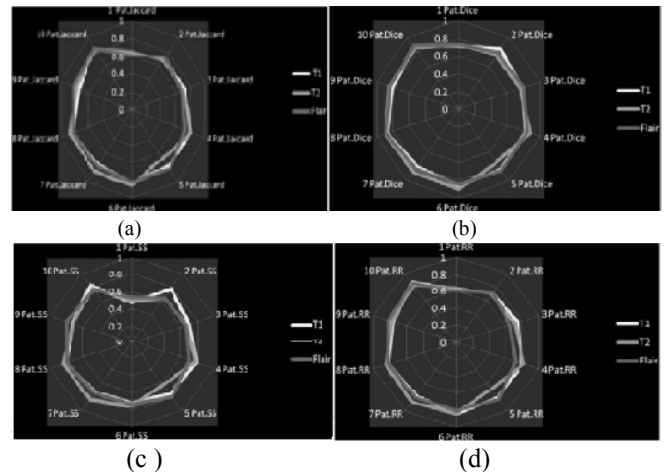


Fig. 5 plot of similarity metrics for ten patients in three modalities for (a) Jaccard (b) Dice (c) Sneath and Sokel (d) Russel and Rao (RR)

#### D. Patient independent classifier for PF tumor prediction

Figure 6(a) shows the PC projected feature plots. Note for all three T1, T2, and FLAIR MRI modalities, combination of the three features representing tumor samples are clustered into compact regions, while the non-tumor samples are spread all over. Since we are interested to develop a patient-independent prediction classifier for PF tumor that combines information from all three MRI modalities, all three features are combined from all three MRI modalities. Figure 5(b) shows such plot wherein all nine features are combined and projected onto their first two PCs. We note that the tumor samples are further clustered while the non-tumor regions are increasingly scattered. Such compact cluster of the tumor features is expected to yield better tumor classifier with high TPF while sacrificing less FPF.

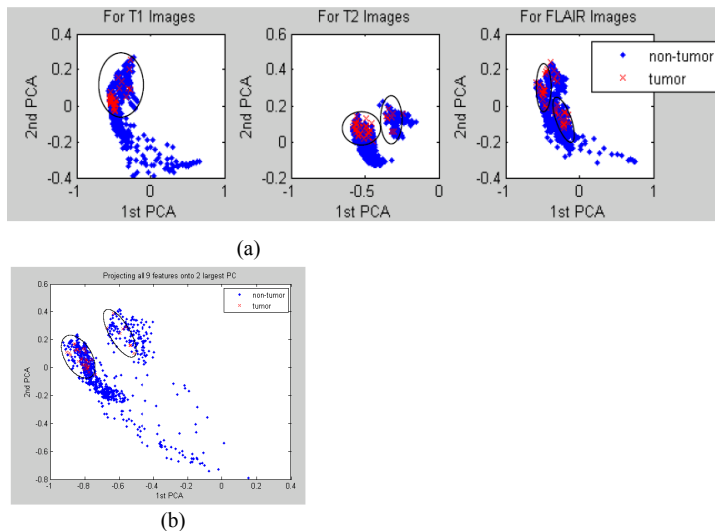


Fig. 6 (a) Projection of 3 features (intensity, PTPSA, MultiFD) onto their first 2 principal components; and (b) Projection of all 9 features (intensity, PTPSA and MultiFD from all 3 MRI modalities) onto their first 2 principal components

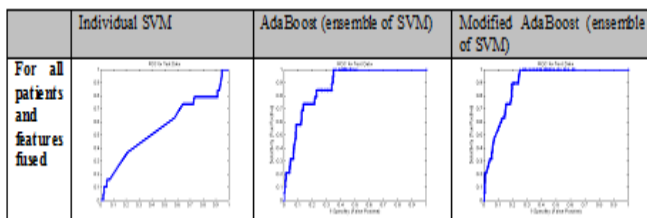


Fig. 7 The ROC when data from all six patients are combined together for different classification scheme.

Figure 7, however, shows the most difficult case wherein data from all patients are combined together in order to obtain a patient independent PF tumor prediction scheme. The ROC plot shows that the modified AdaBoost can achieve TPF = 1 at around FPF = 0.25, while the regular AdaBoost achieve TPF = 1 at around FPF = 0.35. This clear performance gain for the modified AdaBoost verifies the efficacy of the patient-independent PF tumor detection and prediction scheme.

#### Acknowledgements

This work is supported in part by NCI/NIH research grant 1R15CA115464. The authors would like to express appreciation to St. Jude's Children's Hospital and Children's Hospital of Philadelphia for providing the pediatric brain MR images for this work. We also thank Atiq Islam for his help in Classifier simulation.

#### REFERENCES

- [1] A. W.C. Liew and H. Yan, "Current Methods in the Automatic Tissue Segmentation of 3D Magnetic Resonance Brain Images", *Current Medical Imaging Reviews*, Vol. 2, No. 1, 2006.
- [2] Y. Li and Z. Chi, "MR Brain Image Segmentation Based on Self-Organizing Map Network", *International Journal of Information Technology* Vol. 11, No. 8, 2005.
- [3] N. Sarkar, and B.B. Chaudhuri, "An efficient approach to estimate fractal dimension of textural images. *Pattern Recognition*,. 23: p. 1035- 1041,1992.
- [4] K. M. Iftekharuddin, "Techniques in fractal analysis and their applications in brain MRI", Medical imaging systems technology: analysis and computational methods, L. Cornelius T, Editor. World scientific publications, 2005.
- [5] J. M. Zook and K. M. Iftekharuddin, "Statistical analysis of fractal-based brain tumor detection algorithms," *Magnetic Resonance Imaging*, vol. 23, pp. 671-678, 2005.
- [6] Y. Sun, C.F. Babbs, E.J. Delp, "A comparison of feature selection methods for the detection of breast cancer in mammograms: adaptive sequential floating search vs. genetic algorithm", *Engg. In Medicine and Biology Society, IEEE-EMBS 2005, 27<sup>th</sup> Annual International Conf.*, Issue , Page(s) 6532-6535 ,2005.
- [7] M.F. McNitt - Gray, H.K Huang, J.W. Sayre, "Feature selection in the pattern classification problem of digital chest radiograph segmentation", *Medical Imaging, IEEE Transactions on* Vol. 14, Issue 3, page (s) 537-547, Sep.1995.
- [8] N.I. Weisenfeld and S.K. Warfield, "Normalization of Joint Image – Intensity Statistics in MRI using the Kullback – Leibler Divergence" *Biomedical Imaging: Nano to Macro, IEEE International Symposium on Volume*, Issue 15-18 April 2004 Page(s):101-104 Vol.1, 2004
- [9] V. Calhoun, T. Adah and J. Liu, "A Feature – Based approach to combine functional MRI, structural MRI and EEG brain imaging data" *Proceedings of 28<sup>th</sup> IEEE, EMBS Annual International Conference*, 2007 .
- [10] J. Novovicova, P. Pudil and J. Kittler, "Divergence Based Feature Selection for Multimodal Class Densities", *IEEE transaction on Pattern Analysis and Machine Intelligence*, Vol.18, No.2, Feb. 1996.
- [11] K.M. Iftekharuddin, A. Islam, J. Shaik, C. Parra, and R. Ogg, "Automatic brain tumor detection in MRI: methodology and statistical validation," *Proceedings of the SPIE Symposium and Medical Imaging*, vol.5747, pp.2012-2022,2005
- [12] A. Islam, K. M. Iftekharuddin, R.Ogg, F.H. Laningham, and B. Sivakumar, "Multifractal modeling, segmentation, prediction and statistical validation of posterior fossa tumor" *SPIE Medical Imaging Conference*, 2008.
- [13] K.M. Iftekharuddin, J.Zheng, M.A. Islam and R.J.Ogg, "Fractal – based Brain Tumor Detection in Multimodal MRI" *Applied Mathematics and Computation Vol*, 206, 2009
- [14] S. Ahmeed, K. M Iftekharuddin, "Efficacy of Texture, Shape, and Intensity Feature Fusion for Posterior-Fossa Tumor Segmentation in MRI" *IEEE TRAN. ON INF. TECH. IN BIOMEDICINE, To Appear*, 2011.
- [15] B. B Mandelbrot, "The fractal geometry of nature", *San Francisco: Freeman*, 1983.
- [16] K. M. Iftekharuddin, W. Jia and R. Marsh, "Fractal analysis of tumor in brain MR images," *Machine vision and applications*, vol.13, pp. 352-362, 2003.
- [17] K.M. Iftekharuddin, A. Islam, J. Shaik, C. Parra, and R. Ogg, "Automatic brain tumor detection in MRI: methodology and statistical validation," *Proc. of the SPIE Symp. and Med. Imag.*, vol.5747, pp.2012-2022, 2005.